Metallurgical and Materials Engineering *Research paper*
Association of Metallurgical Engineers of Serbia AMES *https://doi.org/10.30544/596*

EFFECT OF HEAT TREATMENT ON HARDNESS AND WEAR RESISTANCE OF HIGH CARBON-HIGH CHROMIUM STEEL (FMU-11)

Alireza Darvishi[1,2,], Aria Daneshmayeh[1, 3], Alihosein Salehi[2, 4], Mahdi Ahmadi[2, 4], Alireza Soleymani[4]*

[1]Graduate School of Materials Engineering, Azad University, Saveh, Iran
[2]Department of Technology, Ravanshir Steel Factory, Takestan, Iran
[3]Department of Production, Ring Khodro Pars Factory, Takestan, Iran
[4]Department of Production, Ravanshir Steel Factory, Takestan, Iran

Received 08.12.2020
Accepted 18.01.2021

Abstract

In the present study, microstructure, hardness, and abrasion resistance of a heat-treated high carbon-high chromium steel (FMU-11) used in the cement mills were investigated. To investigate the best heat-treating cycle for the FMU-11 steel, three sets of samples were heat treated. The first set was tempered two times, the second set was re-hardened, and the third set was cryogenically heat treated. These samples were then compared with the conventionally heat-treated samples. The samples' microstructure was studied using an optical microscope, where traditional black and white etching, as well as color etching, were used. Scanning electron microscopy (SEM) was applied for higher magnification studies and in-depth analysis of the chemical composition. The mechanical properties were investigated by measuring the hardness and the wear resistance for the samples heat-treated in different cycles. The results showed that the cryogenic treatment and double-tempered samples had the highest hardness and wear resistance. In addition, the results showed that the re-hardening operation caused the carbides to be finely separated and evenly distributed in the steel matrix. The wear test results illustrated that the wear mechanism could be the delamination wear and the abrasive wear combined.

Keywords: heat treatment; mechanical properties; wear resistance; cryogenic treatment; cement mill.

[*]Corresponding author: Alireza Darvishi, *Darvishi529@gmail.com*

Introduction

A milling system is one of the most widely used machines for reducing the granular sizes in cement production. The linings used in the cement mills body can be divided into three general categories: the floor liners, the inlet wall liners, and the outlet wall liners. Because of the wear and the impact properties, each category of the liners is different. Choosing the right material for the liners and the right heat treatment for the selected materials are critical in their performance. In the liners used in the walls, abrasion resistance, and in the liners used in the floor, impact resistance are priority properties [1, 2]. Recently, a new type of steel called high carbon-high chromium steel (FMU-11) has been used in the production of cement mill floor liners. This steel contains 1.4-1.6% carbon and 11-13% chromium. This type of chemical composition provides good abrasion resistance, and if a suitable heat treatment cycle is applied to obtain a tempered martensite structure with a minimum amount of retained austenite and uniform distribution of carbides in the steel matrix [3]. If the structure of this steel becomes homogeneous, the possibility of forming chromium carbide in the structure is small. Chromium up to 13.0% can be solved in the austenite, so if the chromium separates and its concentration increases in the separated areas, the possibility of forming carbides increases, and as a result, the impact resistance can be reduced [4]. The ternary interaction of the Fe-Cr-C system (shown in Fig. 1) is of central importance to predict the formation of carbides during the heat treatment of this steel. The ternary system is characterized by the presence of three carbides ($(Fe,Cr)_3C$), M_7C_3, and $M_{23}C_6$, where M could be Cr or Fe. All three carbides show extensive solid solubility with respect to the alloy but are essentially stoichiometric with respect to carbon [5]. Cementite presents in most steels, and the other two carbides are both common in the alloyed steels. However, there is a fourth carbide in the system, Cr_3C_2, that essentially does not dissolve Fe and is of minor importance for this type of steel [5].

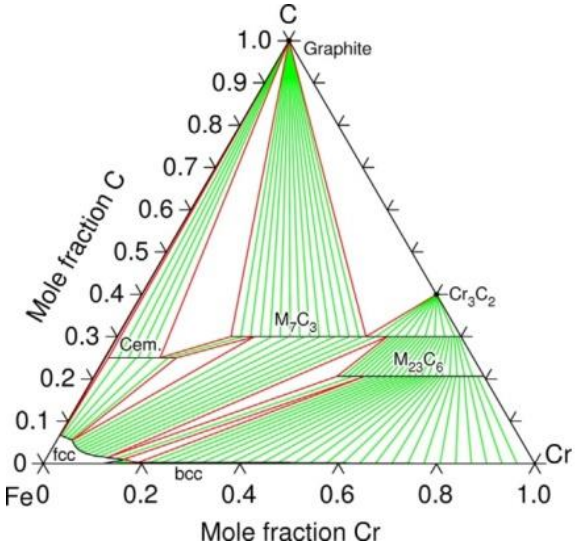

Fig. 1. Isothermal section of the Fe-Cr-C phase diagram at 1000 °C calculated from an evaluated thermodynamic parameter [5].

The high carbon-high chromium steel is characterized by a high-volume fraction of the hard carbides (such as M_7C_3, $M_{23}C_6$, etc.) in the matrix due to its high carbon and high chromium content, giving reasonable tribological properties [6]. Studies have shown that the wear resistivity is strongly dependent on the morphology and distribution of the hard carbides [6]. The solidification of this steel could cause considerable segregation of the alloying elements. The first crystals to solidify would be enriched with iron, carbon, chromium, and other elements that could be rejected to the interdendritic or intercellular liquid regions, where the alloy carbides eventually form [7]. These steels are air hardening type with maximum dimensional stability during heat treatment and offer high hardness and wear resistance [8]. The heat treatment methods suggested for high chromium martensitic steels are:

(a) Austenitization between 950 and 1100 ºC followed by quenching;

(b) Tempering between 200 and 300 ºC for high strength, moderate toughness, and resistance and between 600 and 700 ºC for moderate strength, high toughness [9, 10].

The microstructure of the hardened high carbon-high chromium steel includes primary and secondary carbides retained from austenitization prior to austenite grain boundaries formation. Many of the smaller carbides in the annealed structure could be dissolved during the austenitization. However, the high volume fraction of the retained carbides relatively adheres to the austenite grain boundaries, helping to maintain a fine austenitic grain size, and eventually contributes to the wear resistance of steel. Since the steel matrix consists of tempered martensite and retained austenite, it would be difficult to chemically etch, because of the presence of high chromium content and, even if etched, it would be too fine to be determined in the light microscope [7].

In the reported literature [6, 11], the wear test used to study the wear behavior of the hard phases (such as M_7C_3, $M_{23}C_6$) is mostly restricted to the two-body abrasive wear. Since the surface damage, in the real-scale condition, in the cement mills, caused by fretting action is the result of several wear mechanisms [12], the morphology of the worn surfaces is much more complicated. Therefore, it is important to capture a better understanding of the role of hard phases in the abrasion wear behavior. Studies on the high-carbon-high chromium steel have shown that heat-treating the steel after hardening and tempering at low temperature will not only reduce the retained austenite but also could cause carbides to be decomposed then change the hardness values [4, 13]. Similarly, the studies on the effects of austenite and tempering temperature on the high chromium steels showed that by re-tempering, the remaining austenite could be reduced, and the hardness could be increased with the help of secondary carbide precipitation [14]. Earlier studies revealed that austenitizing at a lower temperature of 950 ºC did not allow a large amount of alloy carbides to go into the solution, leading to the achievement of lower strength and toughness. On the other hand, a high austenitizing temperature of 1100 ºC or above, despite helping in the dissolution of alloy carbides, resulted in an increase in prior austenite grain size besides increasing the δ-ferrite, as well as retained austenite content [15].

There is not much work to investigate this type of steel (FMU-11), knowing its properties, optimal composition and best heat treatment cycle, to be used in the mill crushers and in the cement industry. Due to an increase in the usage of this steel and demand for this sort of application, in this study, different heat treatment cycles were examined on this steel. Then, the influence of heat treatment cycles on the hardness, the

microstructure, and the abrasion mechanism was investigated using different characterization techniques.

Experimental procedure

Test samples used in the current study, sectioned with the dimensions of 25 mm × 25 mm ×150 mm, were prepared from a high carbon-high chromium steel (FMU-11) with the chemical composition determined by the Hilger spectrometer, as shown in Table 1. The steel was melted using an induction furnace and then poured into a silica sand mold.

Table 1. Chemical composition of high carbon-high chromium steel (FMU-11).

C	*Si*	*Mn*	*Cr*	*Mo*	*V*	*S*	*P*	*Fe*
1.4	*0.38*	*0.69*	*11.71*	*0.29*	*0.039*	*0.017*	*0.008*	*Balance*

Table 2 shows different heat treatment conditions applied to the samples. Before the heat treatment, the surface of the samples was coated with cupric sulphate ($CuSO_4$) to prevent oxidation and de-carburization. Due to the low heat transfer coefficient of this steel [7], the samples were heated to 650 ºC, with a heating rate of 70 ºC/h, and after keeping them there for 30 minutes, they were isothermally treated at 1000 ° C, with a heating rate of 100 ºC/h. At this temperature, the samples were kept for 0.5 minutes per mm of thickness, followed by a direct quenching process in the compressed air environment. After the heat treatment, the samples were coded according to Table 2 and subjected to other characterizations for this investigation.

Table.2 Heat treatment cycle of samples.

Name	T3	H3	D4	K3
Heat treatment	*Once tempered at 250 ℃.*	*Re-hardened at 1000 ° C.*	*Tempered two times at 250 °C and 550 °C.*	*Tempered at 250°C and 550 °C and cryogenically treated to -70 °C for 168 hours.*

For the microstructural analysis, samples were prepared based on the ASTM E3 standard [16]. To etch of the samples, different colors, black and white etchants have been tried in accordance with the ASTM E407 standard [17]. Among different etchant solutions tried, Beraha'sCdS color reagent displayed the most obvious microstructure. The optical micrographs were prepared according to the ASTM E883 standard [18], using an optical microscope (Nikon MA200). The scanning electron microscopy (SEM) was also utilized to prepare micrographs using Vega Tescan setup. The amount of retained austenite and volume fraction of carbides (primary and secondary carbides) in the steel matrix was then, calculated by using *CLEMEX* software. XRD analysis (Philips, Xpert, Netherlands) was, additionally, performed to confirm the obtained microstructural results.

The microhardness test was measured according to ASTM E384 standard [19], using MHT-10 with Olympus Bx60 microscope. Hardness test (Hardness Vickers) was performed according to ASTM E18 standard [20]. Finally, the samples were prepared under pin-on-disk wear test, with a load of 200 KPa on the surface of a Sic disk at an

ambient temperature of 10 m/min, with a distance of 3000 m. This test was done according to the ASTM G-99 standard [21], simulating the real conditions in the cement mills. Each wear test at every given load and sliding velocity was repeated three times, and then the average value was reported.

Results and discussion

Microstructure

Fig.2 shows the microstructure of the steel after austenitization at 1000 °C in two different magnifications. As shown in Fig.2-a, there is a non-uniform distribution of the primary carbides in the martensitic field with some retained austenite. The small carbides and martensite needles were clearly seen after this heat treatment. After austenitizing at 1000 ºC, the austenite fraction, calculated by CLEMEX, software was very high (38%). The measured hardness in this stage was as low as 498 HV.

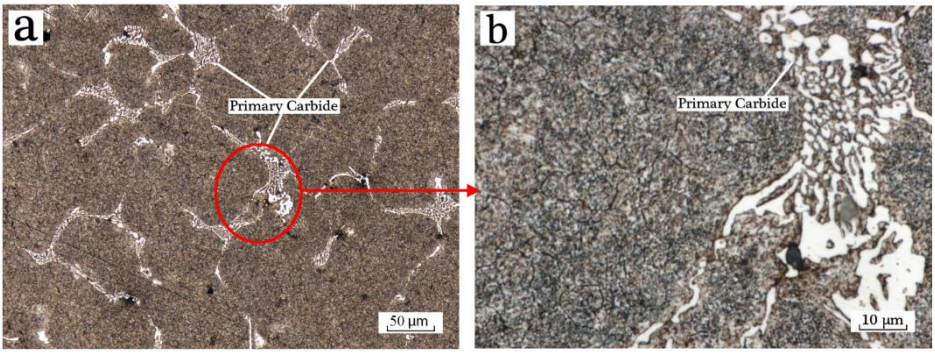

Fig. 2. As-quenched microstructure of FMU-11steel revealed martensite matrix and primary carbides appearing white.

Generally, several carbides with various sizes were likely to form in the final heat-treatment process. The iron-uniform distribution was inhomogeneous, and the size range was quite wide, which caused some defect in the microstructures [5, 22]. As it can be seen from Fig.2, after austenitizing, the microstructure contains primary carbides, and the retained austenite was surrounded by the martensitic structure. Based on the amount of carbon and chromium in this steel, the type of carbides could be determined with the ratio of chromium to carbon. If this ratio is greater than 3, M_7C_3 and $M_{23}C_6$could be formed, and if this ratio is less than 3, M_3C type could be formed in the matrix [22]. Hence, by referring to equation1 and X-ray diffraction (XRD) results shown in Fig. 3, the carbides could be mainly M_7C_3 and $M_{23}C_6$.

$$\text{Carbides type} = \frac{\%Cr}{\%C} = \frac{11.71}{1.4} = 8.36 \qquad 1$$

The XRD line profiles in Fig.3 appear to suggest the presence of M_7C_3 and $M_{23}C_6$ (M could be Fe, Cr, and Mo) carbides, austenite (γ), and martensite (α), after this heat treatment. The volumetric fraction of all dispersed carbides was calculated 5.4% by the CLEMEX software. As shown Fig.3, the concentration of the alloying element between primary carbide is high, and austenite has stabilized. Also, α value shows the

martensite existed in the steel matrix. Microhardness of the primary carbides and matrix was measured to be 1280 HV and 725 HV, respectively. These results could have confirmed the type of carbides formed in the matrix, as explained [23]. The regions near the eutectic carbides were free from precipitates, as their carbon and chromium contents were lower than the average. This point also indicated that the austenitizing time was not enough to completely homogenize the austenite. The high hardenability of this steel has stopped the formation of perlite in the cooling condition under compressed air, lead to the formation of martensite and retained austenite. As the volumetric fraction of eutectic carbides had not been modified during these thermal treatments, the microhardness of the dendritic phase was the most useful parameter to confirm the microstructural evolution [23, 24,25].

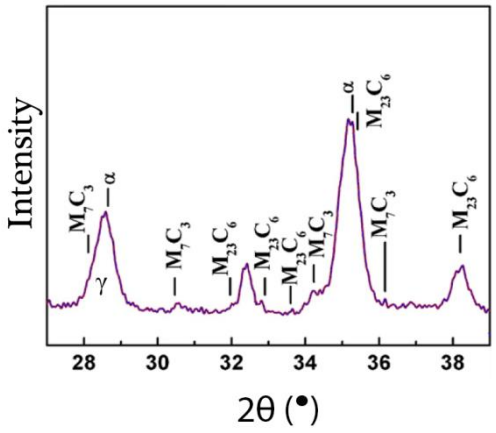

Fig.3. X-ray diffraction line profiles of the sample after austenitized at 1000 °C.

Fig.4 and Fig. 6 show the microstructure of the samples using optical and scanning electron microscope (SEM) analysis, respectively.Fig.5 shows the retained austenite was formed after the following heat treatment cycles. The etching used in this experiment was Beraha'sCdS color reagent solution by which the austenite, the martensite, and the carbides were identified as white, brown, and blue areas, respectively [22, 26, 27]. Due to the low tempering temperature and the presence of the austenite, the T3 sample is shown to be resistant to the transformation of austenite to martensite, and it had high amounts of austenite in the matrix (Fig. 4-a and Fig. 5).

Fig. 4-b shows the presence of the small carbides embedded in the dendritic structure, which have precipitated during the solidification. Because double austenitizing at the high temperatures, the eutectic and small carbides entered the solution, then the austenite was enriched. This happened because of the presence of carbon and chromium that increased the quenchability of the steel alloy. This also ensures the stability of austenite and helps the eutectic to become smaller. The amount of carbides decreased after the second austenitization (Fig. 7-a). In the H3 sample, the size and number of the undissolved carbides were lowered compared to the T3 sample prepared by the single austenitizing heat treatment. These undissolved carbides provide

abundant nucleation sites for the austenite nucleation during the second austenitization treatment, resulting in a finer grain size [28].

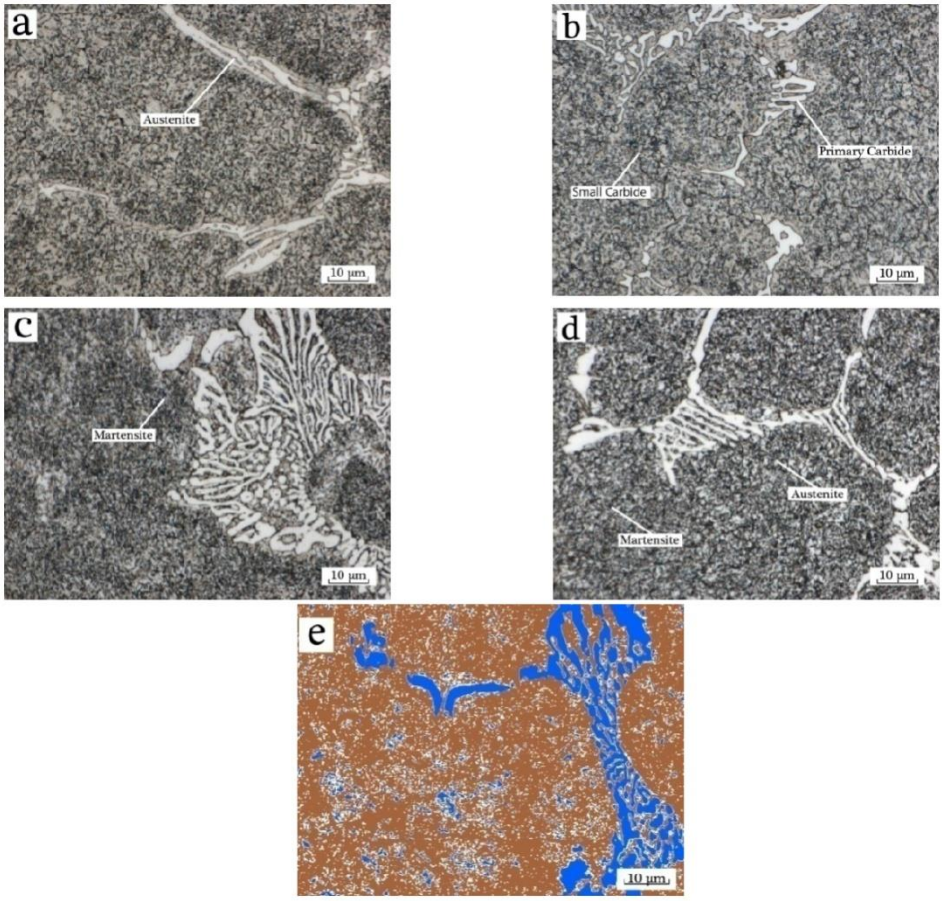

Fig.4. Optical images of samples: a) tempered one time at 250°C (T3), b) Re-hardened at 1000 °C (H3), c) tempered at 250°C and 550 °C and cryogenic treatment was then done at -70 °C (K3), d) tempered two times at temperatures of 250 and 550 (D3), e) T3 sample etched with Beraha'sCdS color reagent (this image was modified with Photoshop software to show the carbides regions).

The SEM images shown in Fig. 6 shows that the only difference between the two samples, T3 and H3, was the fine-grained carbides. During the re-hardening and austenitization at 1000 °C temperature, the primary carbides were decomposed, and during the cooling and tempering, they were converted into fine-dispersed carbides in the structure [7]. As shown in Fig.8 the concentration of the alloying elements such as Cr and Mo in the grain boundaries was higher than in other regions. In addition, the presence of high concentration of Cr and Mo in some regions results in the precipitation of complex Cr-Mo carbides. The energy-dispersive X-ray spectroscopy (EDS) analysis for point A showed the presence of 39.01% of chromium and 51.34% of iron in the

primary carbides. This analysis would confirm the formation of the M_7C_3carbide in that region [7, 13]. The analysis of the points indicated by B and C, also showed that there is a high amount of iron that caused the microhardness reached to 750 HV. Comparing with the microhardness of the martensite it could be concluded that the area is surrounded by the martensitic structure [29].

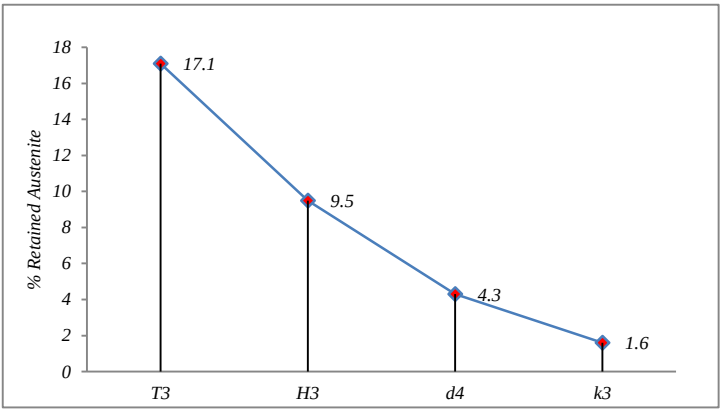

Fig. 5. Retained austenite content variation in the samples (T3, H3, D4, K3) heat treated in different conditions.

An optical micrograph of the sample (K3) heat-treated in the cryogenic environment exhibits the presence of large elongated white areas of primary carbides (Fig. 4c). These carbides were small and nearly spherical in the white regions of large secondary carbides. The tiny black patches of small secondary carbides in the tempered martensite matrix were revealed after etching, shown in Fig. 4 c. The occurrence of secondary carbides in two different size groups, namely large secondary carbides and small secondary carbides, was earlier reported by the authors [26] and is subsequently reaffirmed in different tool steels by other researchers [30, 31]. Comparison of the SEM micrographs of the cryogenic heat-treated sample (K3) shown in Fig. 6c, and conventionally heat-treated sample (T3) is shown in Fig. 6a. It was illustrated that one of the major microstructural modifications by the cryogenic treatment is the variation in the characteristics of ultrafine secondary carbides. This microstructural modification leads to having small secondary carbides. A similar comparison with the EDS taken from the bulk samples (Fig.8) infers that the other significant microstructural alteration imparted by the cryogenic treatment is the substantial reduction in the retained austenite content. The EDS analysis of the extracted carbide particles assisted in concluding that in both conventional heat treatment and cryogenic treatment samples, the secondary carbides are mainly $M_{23}C_6$ while primary carbides are eutectic M_7C_3 (M could be Fe, Cr, and Mo) with a small amount of Cr_7C_3 carbides.

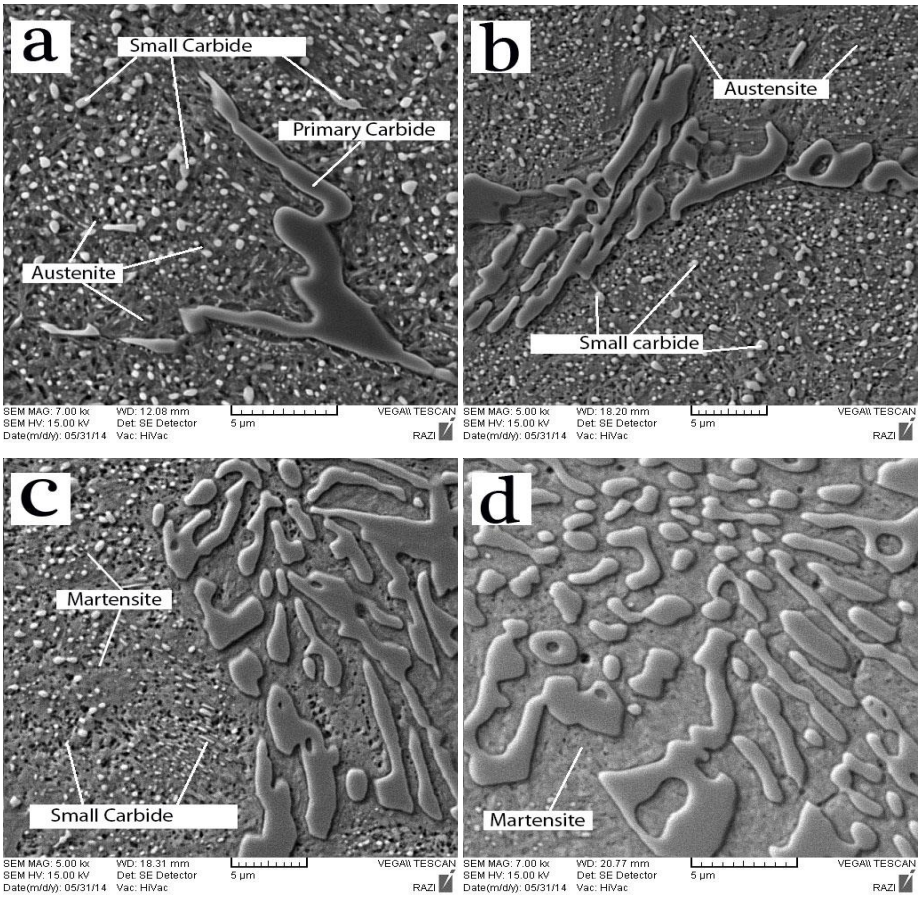

Fig. 6.SEM images of the samples a) T3-tempered one time at 250 °C, b) H3- Re-hardened at 1000 ° C, c) D4-tempered twice at 250 and 550 °C, d) K3-tempered at 250°C and 550 °C, then cryogenic treatment was performed in -70 °C for 168 hours.

In the double-tempered sample (Fig. 4-d and 6-c), the amount of martensite increased, and the retained austenite has decreased (Fig. 5). The second tempering treatment barely modifies the dendritic primary carbides, but that is needed to completely transform the retained austenite. With compares, the microstructure of D4 and other samples revealing very uniform structures is obtained with double tempering. Fine-structured tempered martensite microstructure can be detected in this sample. The etching behavior of the iron matrix was rather uniform, indicating that apparently, the amount of retained austenite is low. As can be seen from Fig.5, the amount of retained austenite in the K3 sample is very small. But, the same points for the T3 and H3 samples, which tempered, compared to the D4 sample showed more retained austenite. In fact, the secondary tempering or freezing process converted the austenite to the martensite [7]. The martensite phase in Fig.6 seems to be a plate-like structure, due to their lenticular shapes and zigzag pattern of small plates [32]. Retained austenite was very stable in high carbon-high chromium steel [7] and did not decompose completely

before reaching temperatures above 500 °C. Therefore, it was observed that between the two samples (T3 and D3) performed two-stages tempering has caused the amount of retained austenite to be drastically reduced.

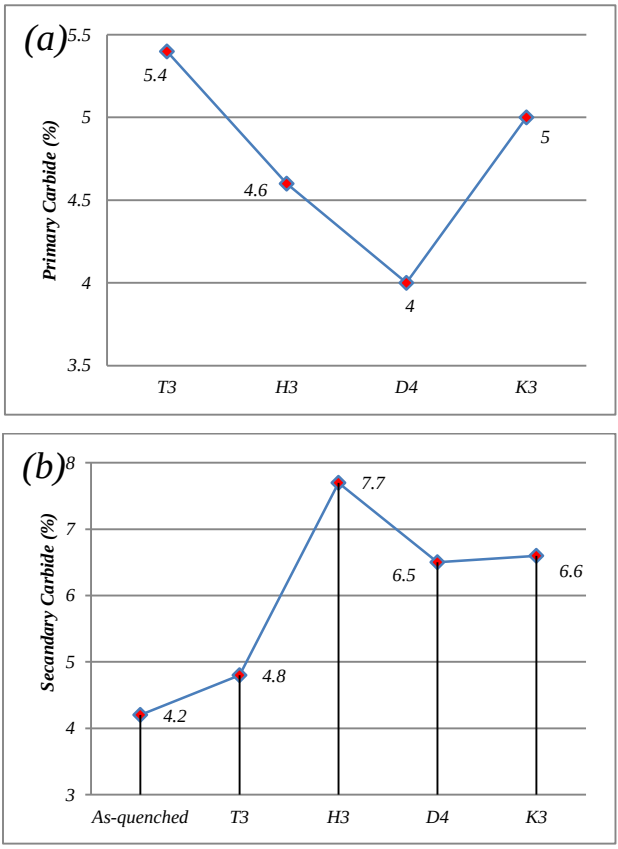

Fig.7. Volume fraction calculated with ± 2% confidence deviation of a) Primary carbides b) Small Carbides.

Hardness

The hardness of the as-cast and compressed air-cooled samples was measured to be 372 and 498 HV, respectively. The results of macro-hardness show that performing cryogenic treatment will not only remove the retained austenite but also increase the amount of secondary hardness. Improvement of the bulk hardness of the selected steel by cryogenic treatment is due to the reduction of retained austenite content and increase in the amounts of secondary carbides and tempered martensite. The estimated microhardness values should be considered only as an apparent index of matrix strength because it is inherently influenced by the small secondary carbide's particles [33].

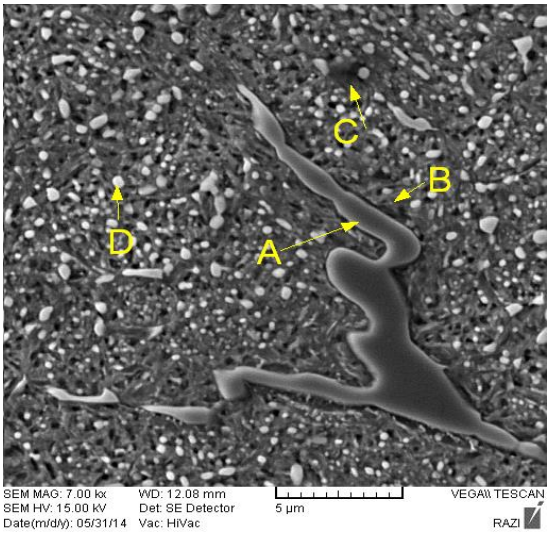

A Zone Element	wt%	B Zone Element	wt%	C Zone Element	wt%	D Zone Element	wt%
C	5.22	C	-	C	-	C	1.75
Cr	39.01	Cr	11.01	Cr	12.71	Cr	10.46
Fe	51.34	Fe	86.84	Fe	85.13	Fe	87.41
Mo	2.79	Mo	1.26	Mo	0.52	Mo	-
Mn	1.63	Mn	-	Mn	1.13	Mn	0.38

Fig. 8. EDS analysis of T3 sample.

Only marginal reduction of fracture toughness value was detected by the cryogenic treatment (K3) over the conventional heat treatment (T3), despite almost complete removal of retained austenite by the former treatment. This is attributed to the higher absorption of energy for the formation of more numbers of micro-voids by decohesion of the small secondary carbide particles [33]. Increasing the hardness for the double austenitized sample (H3) compared to the conventionally heat-treated sample (T3) could be attributed to the dispersion and slicing of the primary carbides. This also could be attributed to the reduction of the carbon content in the steel matrix, the increase in martensite start (M_S) temperature, and creation of secondary hardness [34]. The increased microhardness by the samples prepared by tempering twice (D4), compared to the conventional treatment (T3), is attributed to the complete transformation of the soft austenite to the hard martensite with concurrent enhancement of the hard-secondary carbides. When the sample was tempered twice, most of the retained austenite changed to the martensite and an increase in the hardness was observed. Decomposition of the chromium carbide may also have contributed to the increase in the hardness. Microhardness is an apparent indication of the strength of the matrix because it inherently accounts for the influence of small secondary carbides [35].

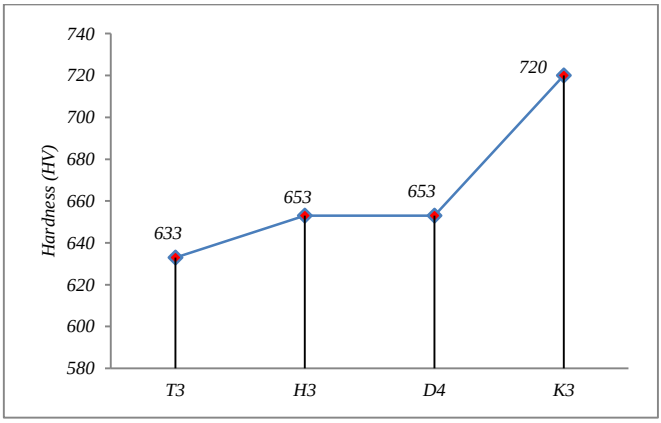

Fig. 9. Macro-hardness of samples after heat treatment.

Wear resistance

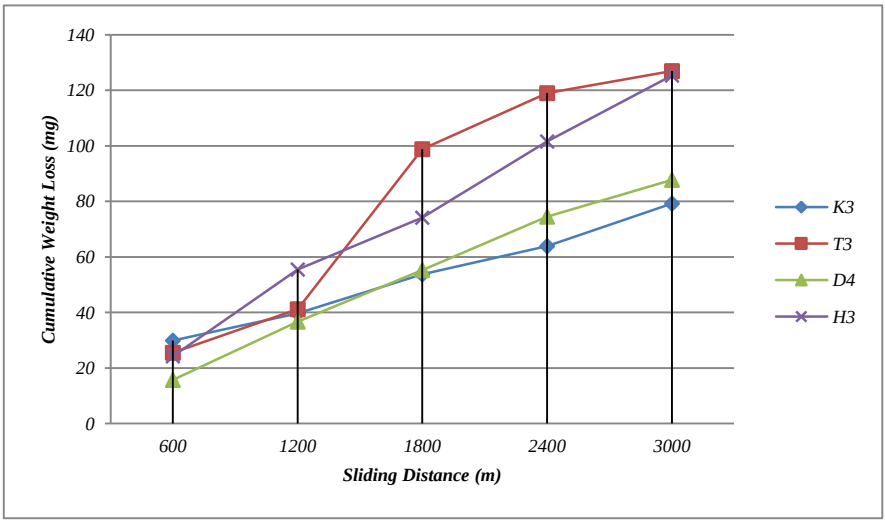

Fig. 10. Cumulative weight Loss of samples as a function of sliding distance.

In Fig.10, the abrasion results for each sample are plotted showing a reduction in the sample weight in terms of slip distance. As these diagrams show, up to 1200 m is related to the RUN-IN stage, in which there is interference between the weight losses of the samples. At the beginning of wear, due to the presence of rough surfaces, the actual contact surface is much less than the nominal contact surface. Therefore, due to the increase in pressure in the actual areas under wear conditions, the wear rate increased. At this stage, due to the presence of unevenness in the surface, the surface oscillation increased. As the slip distance increased, the surface roughness and protrusions were gradually disappeared. The surface became smoother, and the actual contact surface

became approximately equal to the nominal contact surface. As the slip continues, the unevenness of the surfaces decreased and after approximately 1200 to 1800 meters (depending on the type of sample and the abrasion force), the abrasion entered the second stage. The lower slope in the second region could be the result of the reduction of surface roughness and the increase of the actual contact area of the pin [36].

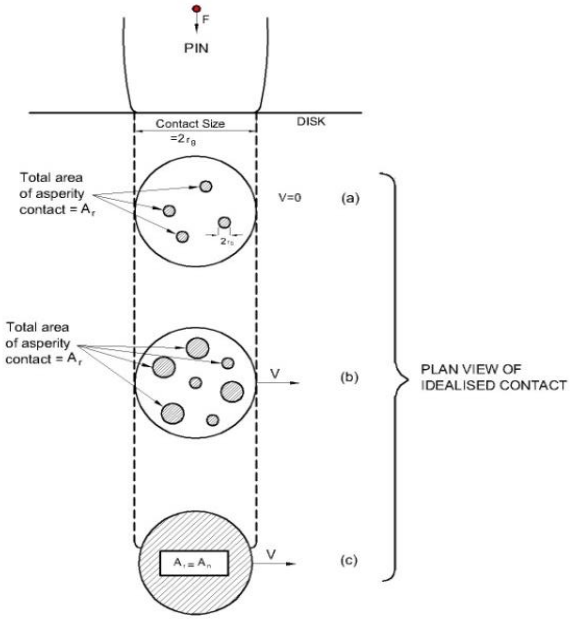

Fig. 11. Schematic of the process of gradually increasing the actual contact surface with increasing slip distance [36].

In the present study, the nature and morphology of the worn surfaces were studied by SEM analysis for all the samples subjected to the test conditions. The measured wear rate of K3 sample is found to be considerably higher than that of other samples. The wear rate of all samples increased linearly with load obeying classical Archard law of wear [37] that could be used to calculate the wear resistance, taken as a reciprocal of wear coefficient [33]. Under the investigated wear conditions for all samples, worn surfaces exhibited rough and metallic luster with the presence of fractured ridges and subsurface cracking, while the generated wear debris were found to be large platelet-shaped metallic particles (Fig. 12 a-d). Fig.12 shows the representative appearance of worn surfaces in the pin-on-disk abrasion test when silicon carbide is used as abrasive. The long scars show that cutting and grooving by the abrasive particle occurred on the surface of the sample. The wear surface appeared heavily deformed and smeared. Comparing the hardness of the SiC [38] with the carbides, the abrasive particle can cut off the specimen effectively. Figures also show the ploughing mode where a groove is formed, which has ridges on both sides, but no wear debris is formed. Fig.12 also assists in illustrating the wear mechanism for the samples subjected to the wear test. The mechanism of wear for the conventional heat-treated sample (T3) sample was

deformation-induced delimitation wear [39]. This has been evidenced by the rough metallic nature of the worn surface, the presence of the deformed edges and the large deformed layer of the worn surface propagated parallel to the sliding direction. Due to the formation of discontinuous particles and chips, and almost removal of the entire material on the surface it seemed that the predominant wear mechanism in both H3 and K3 samples was the abrasive wear mechanism. In these samples, wear occurred with the surface damage due to the presence of hard particles at the interface of the two surfaces slide relative to each other. In this wear stage, the second phase (particle) was able to scratch the samples slowly. The wear mechanism for the D3 sample under the investigated wear test condition was a combination of delamination and abrasion wear [40]. Fig. 12-c assist in inferring that the extent damage of the worn surface, degree of plastic deformation of subsurface and the size of the generated wear debris decreased in the order of conventionally heat treated (T3 sample).

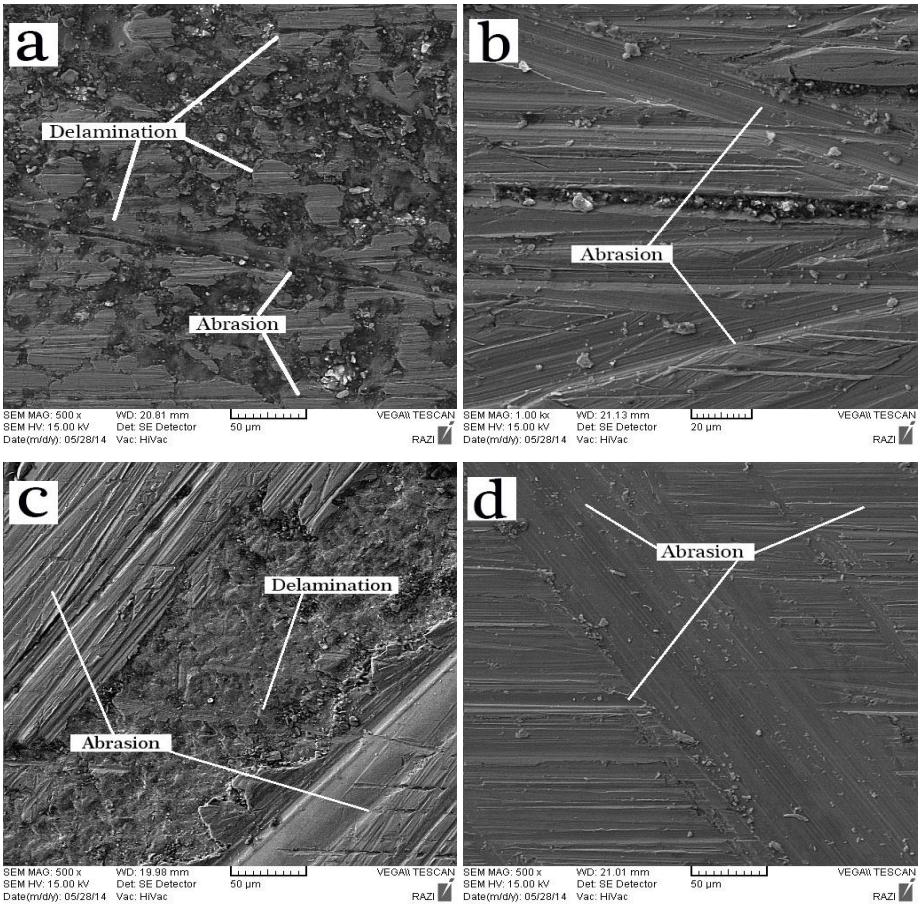

Fig. 12. Electron microscope images of worn surfaces. a) sample T3 tempered at 250 °C, b) sample H3 re-hardened at 1000 ° C, c) sample D4tempered twice at 250 and 550 °C, d) sample K3 tempered at 250°C and 550 °C, then cryogenically treated at -70 °C for 168 hours.

The pin on disk test results also shows that increasing the retained austenite content leads to greater wear rates with garnet as the abrasive (Fig.5 and Fig.10). According to the literature [41], it has been shown that increasing the retained austenite content decreases the abrasive mass loss. During air cooling, carbon partitioning to the austenite will take place from the "ferrite" (martensite). Since retained austenite would be expected to be of relatively low carbon content the hardness of any martensite that formed through deformation induced transformation would also be low due to its low carbon. During the abrasion process, the matrix was preferentially removed; the rate of removal of the matrix controlled the extent to which the carbides became exposed and fractured. The increase in hardness of the matrix offers stronger support for carbides to inhibit its spalling and prevents large grooves from forming during abrasion wear. In addition, the secondary carbides which precipitate in the matrix regions of high chromium iron also influence the abrasion behavior.

Conclusions

The following conclusions could be drawn from an investigation on the high carbon-high chromium steel (FMU-11), heat-treated under different conditions.

i. The morphology of carbides became finer during re-hardening heat treatment of FMU-11 steel.
ii. FMU-11 steel in the cryogenic treatment condition exhibited the highest abrasive wear resistance, which was attributed to the martensitic microstructure with the finer morphology of carbides.
iii. The cryogenic treatment caused almost complete removal of the retained austenite for FMU-11 steel.
iv. Microstructural modifications by cryogenic treatment increased the wear resistivity of FMU-11 steel.
v. The morphology of carbides became coarser with increasing tempering temperature during the multiple tempering treatments of FMU-11 steel.
vi. After two tempering treatments and quenching, the microhardness and wear resistance were increased.

Acknowledgments

The authors are thankful to the management and staff of Ravanshir Steel Factory (RSF) and Ring Khodro Pars (RKP) for their cooperation and facilities in this investigation.

References

[1] P.W. Cleary: Minerals Engineering, 14 (2001) 1295-1319.
[2] S. Banisi, M. Hadizadeh: Minerals Engineering, 20 (2006) 132-139.
[3] ASM Metal Handbook, Heat treating, 9th Ed, ASM, New York, 1991, 160–290.
[4] Das. D, Ray. K.K: Philosophical Magazine Letters, 92 (2012) 295-303.
[5] Alexandra V. K, Hallstedt B, Christoph Broeckmann: Calphad, 46 (2014) 24-33.
[6] K. Singh, R.K. Khatirkar, S.G. Sapate: Wear, 328–329 (2015) 206–216.
[7] Roberts G, Krauss G, Kennedy R, Heat Treatment and Processing Principles, 5th Ed, American Society for Metal, New York, 1990, 203-217.
[8] Surberg, C.H., P. Stratton, K. Lingenhöle: Cryogenics, 48 (2008) 42-47.

[9] Balan, K., A.V. Reddy, D. Sarma: Materials engineering and performance, 8 (1999) 385-393.
[10] Rajasekhar A, G.M. Reddy: Materials Design and Applications, 224 (2010) 9-18.
[11] Salunkhe. S, Fabijanic. D., Nayak. J, Hodgson. P: Materials Today, 2 (2015) 1901–1906.
[12] J.J. Coronado, S.A. Rodríguez, A. Sinatora: Wear, 301 (2013) 82–88.
[13] J.D. Lemm, A.R. Warmuth, S.R. Pearson, P.H. Shipway: Tribology International, 81 (2015) 258–266.
[14] D. Das, K.K. Ray: Materials Science and Engineering, 541 (2012) 45– 60.
[15] I. Souki, D. Delagnes, P. Lours: Procedia Engineering, 10 (2011) 631-637.
[16] ASTM Standard E 3-01, ASTM International, (2001) 1-12.
[17] ASTM Standard E 407-99, ASTM International, (2015) 1-21.
[18] ASTM Standards E883 – 02, ASTM International; (2017) 1-17.
[19] ASTM Standards E384 - 08, ASTM International, (2008) 1-33.
[20] ASTM Standards E 18-03, ASTM International, (2003) 1-22.
[21] ASTM Standards G 99-05, ASTM International, (2005) 1-5.
[22] B.-J. Lee: Calphad, 16 (1992) 121–149.
[23] K. Fukaura, Y. Yokoyama, D. Yokol, N. Tsujii, K. Ono: Metallurgical and Materials Transactions A, 35 (2004) 1289-1300.
[24] S. Chabour, G. Cizeron: Fonderie Fondeurd Aujourd'hui, 175 (1998) 42.
[25] V. Lanteri, C. Thomas, J. Bocquet, H. Yamamoto, S. Araya, In: Proceedings of The 7th International Conference on Steel Roling, Chipa, Japan, The Iron and Steel Institute of Japan, 1998, 423-425.
[26] B.L. Bramfitt, A.O. Benscoter, Metallographer's Guide, First Ed, ASM International, Ohio, 2002, 45-215.
[27] E. Beraha, B. Shpigler, Color Metallography, First Ed, American Society for Metals, Ohio, 1977, 1-160.
[28] S. Salunkhe, D. Fabijanic, J. Nayak, P. Hodgson: Materials Today, 2 (2015) 1901–1906.
[29] G. Laird, R. Gundlach, K. Röhrig, Abrasion-Resistant Cast Iron Handbook, Third Ed, American Foundry Society, Illinois, 2000, 177.
[30] D. Das, A.K. Dutta, K.K. Ray: Wear, 267 (2009) 297-309.
[31] M.A Jaswin, D.M. Lal, A. Rajaduri: Tribol Trans, 54 (2011) 341-350.
[32] G. Krauss, Tempering and structural change in ferrous martensitic structures, In: Proceedings of an International Conference, Marder A.R, USA, 1984, 101–123.
[33] D. Das, A.K. Dutta, K.K. Ray: Mater Sci and Eng, 527 (2010) 2182-2193.
[34] K. Balan, A.V. Reddy, D. Sarma: Materials Engineering and Performance, 8 (1999), 385-393.
[35] D.N. Collins, J. Dormer: Metal Science and Heat Treatment, 3 (1997), 71-74.
[36] S.C. Lim, M.F. Ashby: Acta Metallurgical, 35 (1987), 1-24.
[37] J.F. Archard: Applied Physics, 24 (1953) 981.
[38] N.P. Suh: Wear, 44 (1977) 1–16.
[39] R.C.D. Richardson: Wear, 11 (1968), 241.
[40] A. Cheikh Larbi, A. Cherif, M.A. Tarres: Wear, 258 (2005) 712.
[41] M. Smith, M.Sc Thesis, University of the Witwatersrand, Johannesburg, 1994